

Modular-based modeling of electric vehicle thermal management system

Modular system implementation in Simulink

Master's thesis in Applied Mechanics and Sustainable Energy Systems master programs

Babak Heydarnezhad Karimi, Noah Wirsén

MASTER'S THESIS 2021:22

Modular-based modeling of electric vehicle thermal management system

Modular system implementation in Simulink

Heydarnezhad Karimi, Wirsén



CHALMERS
UNIVERSITY OF TECHNOLOGY

Department of Mechanics and Maritime Sciences
Division of Vehicle Engineering and Autonomous Systems
CHALMERS UNIVERSITY OF TECHNOLOGY
Gothenburg, Sweden 2021

Modular-based modeling of electric vehicle thermal management system
Modular system implementation in Simulink
HEYDARNEZHAD KARIMI, WIRSÉN

© HEYDARNEZHAD KARIMI, WIRSÉN 2021.

Supervisor: Hamed Jamshidi, Volvo Cars
Examiner: Jelena Andric, Division of Vehicle Engineering and Autonomous Systems

Master's Thesis 2021:22
Department of Mechanics and Maritime Sciences
Division of Vehicle Engineering and Autonomous Systems
Chalmers University of Technology
SE-412 96 Gothenburg
Telephone +46 31 772 1000

Cover: Thermal management system in an electric vehicle
Department of Mechanics and Maritime Sciences
Printed by Chalmers Reproservice
Gothenburg, Sweden 2021

Modular-based modeling of electric vehicle thermal management system
Modular system implementation in Simulink
BABAK HEYDARNEZHAD KARIMI, NOAH WIRSÉN
Department of Mechanics and Maritime Sciences
Chalmers University of Technology

Abstract

There are many advantages coupled to the transition from conventional internal combustion engines (ICEs) to battery electric vehicles (BEVs). From an environmental standpoint, BEVs are generally associated with less emissions, resulting in cleaner air in cities and lower contribution to climate change. To replace the ICEs, the energy efficiency of a BEV needs to be maximized. If that regard, an optimized thermal management system plays a vital role.

Thermal management system ensures not only higher energy efficiency but also longer range, increased lifespan of the internal components, reduced running cost, etc. This project aims to develop a novel modeling methodology for the BEV thermal management from the system perspective. The goal was to perform simulations at low computational costs while capturing the relevant physics of the system with good accuracy. The work comprised several steps: become familiar with the existing thermal management system, collecting data from simulations, experiment and supplier, processing data in the form of regression, model the data in a system format for different boundary conditions and finally validate the system for different driving scenarios and ambient conditions. In this methodology, three physical properties are considered: mass flow rate and pressure to validate the system from a fluid perspective; and temperature to consider the thermal aspect.

A component-based modeling approach was employed making it possible to capture the behaviour of the individual components and their interactions. The approach is very robust since once the components properties are mapped, the model can be used in multiple thermal management layouts.

The developed model was successfully validated from the flow perspective with the pump component having the biggest impact in the model performance. The pumps were modeled with high accuracy within 5 % error margin, and the system produced accurate results for mass flow rate, temperature and pressure. The thermal validation was performed for different driving scenarios such as highway, city driving and WLTC. The system followed similar trends in the mass flow rate, temperature difference and pressure drop over each component compared to GT-SUITE simulations. The model has great potential to serve as a virtual test bench for different design concepts. The usage of the model will substantially reduce the simulation time and efficient optimization procedures, during both physical and virtual testing.

Keywords: BEV, Simulink, GT-SUITE, Thermal management system, Driving cycle, Cooling system, Modular approach.

Acknowledgements

Already from day one, our colleagues at Volvo Cars have been friendly and welcoming. They have constantly been supporting us with their expertise and knowledge in the field of automotive engineering.

We would especially like to extend a warm thank you to our supervisor Hamed Jamshidi who played a vital role in the progression of this thesis. He has inspired us with ideas. With Hameds help, we have gained experience and an innovative spirit to solve complex problems.

We would also want to direct a thank you to Juan Gómez, who has given us valuable feedback and IT-support during this project.

Lastly, we would like to express our gratitude to our examiner Jelena Andric, for her feedback and comments. She has brought us guidance and advice throughout the thesis. She has also provided helpful material for this project.

Babak Heydarnezhad Karimi, Noah Wirsén, Gothenburg, June, 2021

Nomenclature

Abbreviation List

AC	Alternative Current
BEV	Battery Electric Vehicle
CC	City Cycle
CFD	Computational Fluid Dynamics
CPU	Central Processing Unit
CS	Cooling System
DC	Direct Current
ED	Electric Drive
EFAD	Electric Front Axial Drive
ERAD	Electric Rear Axial Drive
EV	Electric Vehicle
Fig.	Figure
GT	GT-Suite
HW	Highway
ICE	Internal Combustion Engine
IEMF	Inverter Electrical Module Front
IEMR	Inverter Electrical Module Rear
OBC	On Board Charger
TCS	Thermal Cooling System
VCU	Vehicle Control Unit
WLTC	Worldwide Harmonized Light-Duty Vehicles Test Procedure

Symbol List

Nomenclature

α	Thermal diffusivity	$(\frac{m^2}{s})$
ΔP	Pressure difference	(kPa)
ΔT	Temperature difference	(K)
Δx	Distance between two nodes	(m)
\dot{m}_{in}	Inlet mass flow	$(\frac{kg}{s})$
\dot{m}_{out}	Outlet mass flow	$(\frac{kg}{s})$
\dot{Q}	Flow rate	$(\frac{kg}{s})$
μ	Dynamic viscosity	$(\frac{kg}{ms})$
ν	Flow field velocity	$(\frac{m}{s})$
ρ	Density	$(\frac{kg}{m^3})$
A	Area	(m^2)
C_p	Specific heat capacity	$(\frac{J}{kgK})$
h	Heat transfer coefficient	$(\frac{W}{m^2K})$
k	Thermal conductivity	$(\frac{W}{mK})$
L	Characteristic length	(m)
P_{0in}	Total pressure at the inlet	(kPa)
P_{0out}	Total pressure at the outlet	(kPa)
P_{Loss}	Pressure loss	(kPa)
Pr	Prandtl number	
q	Heat loss	(W)
R_{Flow}	Flow Resistance	$(\frac{Ns}{gm^2})$
Re	Reynolds number	
T	Temperature	(K)
t	Time	(s)

Contents

List of Figures	xiii
1 Introduction	1
1.1 Background	1
1.2 Aim and objectives	1
1.3 Scope and limitations	2
2 Theory	3
2.1 Kirchhoff's Laws	3
2.2 Radiator model	4
2.2.1 Equations for the radiator model	4
3 Method	7
3.1 Introduction	7
3.2 BEV components	8
3.3 Simulink	10
3.4 Data acquisition	11
3.5 Regression	12
3.6 Library in Simulink	16
3.7 Modeling in Simulink	19
3.8 Modeling scenarios	21
3.8.1 Highway driving at 35°C and 15°C	23
3.8.2 City Driving at 46°C	23
3.8.3 WLTC at 35°C and 15°C	23
4 Validation	24
4.1 Steady-state scenario	24
4.2 Transient scenarios	27
4.2.1 Highway Driving at 35°C	27
4.2.2 Highway Driving at 15°C with passive cooling	29
4.2.3 WLTC at 35°C	30
4.2.4 WLTC at 15°C with passive cooling	31
4.2.5 City Driving at 46°C	32
4.3 Remarks from the validation phase	34
5 Conclusion	35

Bibliography	36
A Appendix 1	I
A.1 Source code listing	I

List of Figures

2.1	Kirchoffs analogy for electric and thermal circuit	4
3.1	The three subsystems; Electric Drive Circuit, HV Battery Circuit, Climate Circuit and Cooling Pack	8
3.2	BEV components	8
3.3	Coolant flow rate calculation flow chart	11
3.4	Simulations required	12
3.5	Pressure drops versus mass flow rate in a pipe under various ambient temperatures	13
3.6	Regression for a pipe	14
3.7	Regression for the pump	15
3.8	Library in Simulink	16
3.9	The component EFAD in the Simulink library.	17
3.10	Pressure drop for components that are connected in series	19
3.11	The three subsystems: Electric Drive, Battery and Climate Circuit	20
3.12	State switch in ERAD	21
3.13	Vehicle speed for three different scenarios (highway driving, city driv- ing and WLTC)	22
4.1	Results for the pump inside the HV battery circuit	25
4.2	Results for the pump inside the electric drive circuit	25
4.3	Results for the pump inside the climate circuit	25
4.4	Error comparison for all components at the ambient temperature of 20°C at 100% pump speed.	26
4.5	Error for the mass flow across the two electric machines	27
4.6	Temperature difference in the front and rear electric machines	28
4.7	Temperature difference in the radiator	28
4.8	Error for the mass flow across the battery and radiator	29
4.9	Heat transfer in the radiator and battery	29
4.10	Error for the mass flow across the front and rear electric machines	30
4.11	Temperature difference over the electric machines	30
4.12	Heat transfer in the radiator	31
4.13	Heat rejected from the battery to the coolant	31
4.14	Mass flow error for front and rear electric machines	32
4.15	Temperature difference over the two electrical machines	33
4.16	Temperature difference over the radiator	33

List of Figures

A.1	Error for internal component for 100% pump speed and 0°C ambient temperature	II
A.2	Error for internal component for 100% pump speed and 40°C ambient temperature	II
A.3	Temperature difference over the two inverters in Highway 35°C	II
A.4	Heat dissipated in the radiator for highway at 35°C	III
A.5	Mass flow error in radiator and battery for WLTC at 15°C	III

1

Introduction

1.1 Background

There is a continuous development in the automotive industry, and the shift from fossil to electric has just begun. The implementation of EVs (Electric Vehicles) is a necessity to reduce the emissions that are contributing to climate change, smog, and ecological changes [22]. In order to compete with the traditional internal combustion engines, energy efficiency and driving range are two of the most critical parameters for a BEV (Battery Electric Vehicle)[11]. Several factors affect these two parameters, one of them is the ambient temperature. During cold days, when there is a heating demand, a lot of the energy stored in the battery will be directed towards heating the cabin and the internal components. If the ambient temperature is high, there will instead be a request for cooling. To mitigate the loss in range that arises during these two scenarios, one needs an efficient thermal management system. Improved thermal efficiency will increase the consumer acceptance of BEVs [11]. A thermal management system consists of heating and cooling systems. A cooling system operates by transferring energy away from the internal components. An efficient way of doing this is to transfer energy to the surrounding air by using a cooling pack. This cooling pack is connected to the three subsystems within the BEV; HV (High Voltage) Battery circuit, Electric drive circuit, and Climate circuit. The performance and energy efficiency are directly correlated with the working temperature. By managing the temperature in the system, one mitigates the possibility of fatigue and increases the lifetime of internal components.

1.2 Aim and objectives

The aim of this work is to develop a modeling framework that can be used for virtual testing of different design concepts. The models should be robust (serving multiple purposes), be easy to use and able to run fast. It should be possible to simulate common driving scenarios, perform sensitivity analysis, and optimizations from both hardware and software point of view.

1.3 Scope and limitations

The system is based on the following three properties: mass flow, pressure drop, and temperature. All subsystems are complete from a flow perspective (pressure drop and flow rate) but not from a thermal perspective (temperature). The climate circuit does not contain any thermal models, implying that it can only be studied from a flow perspective. The electric drive circuit and HV battery circuit, on the other hand, both contain thermal models which enable them to be studied from a thermal perspective.

To build a thermal management system, the data that the system is based upon needs to originate from a certain source. The chosen sources for this model are mainly the system simulation software GT-SUITE. However, some of the components are derived from experimental data, CFD in 3D, supplier data, etc. The data needs to be processed before being handled in Simulink. This step is called regression and implies that the studied property is matched to another property with inter-and extrapolation.

2

Theory

This chapter presents how the thermal system is developed and the underlying theory. It describes how the three properties (mass flow, temperature and pressure) are modeled and how they are influencing the system [2].

2.1 Kirchhoff's Laws

A thermal network in a BEV contain flow rates pressure drops and resistances. In an electrical circuit there are currents, voltage drops and resistances. It is possible to make analogy between the two physical domains. The fluid flow in the thermal circuit can be seen as the current flow inside the electrical circuit. The pressure drop/rise can be seen as a voltage drop/rise, and the flow resistance can be seen as the electrical resistance. The similarities between the two circuits are illustrated in figure 2.1. Kirchhoff's laws, nodal continuity and loop equations need to be solved to find the pressure drop and flow rate in the system [2]. A loop in a circuit is any closed path along a circuit that does not encounter the same node more than once.

- Nodal continuity: The sum of the flow rates going in and out from each loop should be zero.
- Loop equations: Sum of pressure changes in each branch around the fluid loop should equal zero.

These two conditions are also exemplified in figure 2.1.

- The current going in and out from a node has to be the same, see figure 2.1a and figure 2.1b.
- The voltage rise in the battery is equal to the summation of voltage drops in the resistors. This implies that the total voltage drop in the circuit has to be zero, see figure 2.1a. A similar statement can be made for the thermal circuit, i.e. the pressure rise in the pump should be equal to the pressure drop in the circuit, see figure 2.1b.

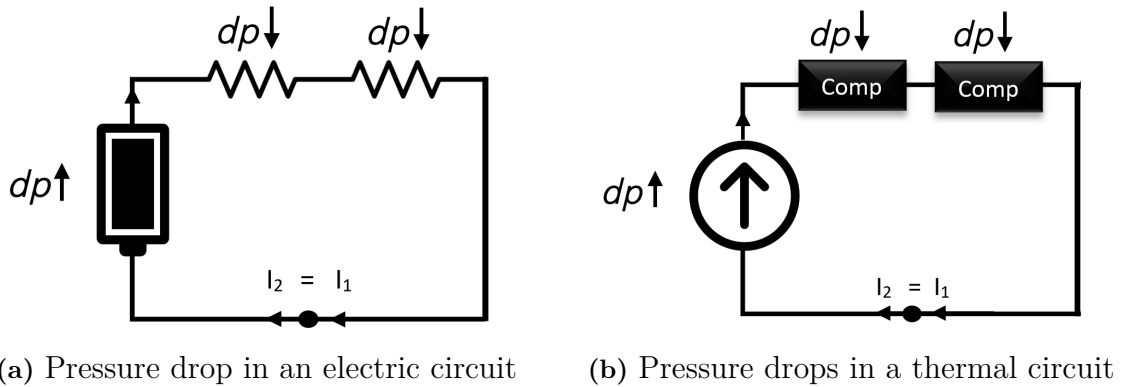


Figure 2.1: Kirchoffs analogy for electric and thermal circuit

The flow resistance can be calculated if the pressure and flow rate across a particular branch is known as:

$$R_{el} = \frac{\Delta V}{I} \rightarrow R_{Flow} = \frac{\Delta P}{Q} \quad (2.1)$$

where R_{Flow} , ΔP and Q is the flow resistance, pressure change and flow rate.

2.2 Radiator model

With Kirchhoff's laws and the analogy between thermal and electric circuits one have solved for two out of three properties (mass flow and pressure). To extract the third property (temperature) one needs to consider the heat transfer in the system.

A central component in a cooling system is the radiator. The working principle of the radiator is to dissipate energy from the coolant gained from the inefficiencies inside the components. This is accomplished by having a different medium (ambient air) at a lower temperature than the coolant. This enables the internal components to function at optimal conditions and mitigate the damage that can arise from thermal fatigue.

2.2.1 Equations for the radiator model

The radiator model, unlike the rest of the components, is a 1D model. A single pipe within the radiator is divided into three nodes (inlet, middle and outlet). Several conditions must be fulfilled to have a physically accurate model. Three of these are the three conservation laws which are summarized in equations 2.2 - 2.4. The conservation laws for mass, momentum and energy for incompressible fluid are described by equations 2.2 - 2.4 [10]:

$$0 = \int_{CS} \rho (\mathbf{V}_r \cdot \mathbf{n}) dA \quad (2.2)$$

$$\sum \mathbf{F} = \int_{CS} \mathbf{V} \rho (\mathbf{V}_r \cdot \mathbf{n}) dA \quad (2.3)$$

$$\frac{dE}{dt} = \int_{CS} e \rho (\mathbf{V} \cdot \mathbf{n}) dA \quad (2.4)$$

Here V_r is the velocity of the in/outgoing flow, \mathbf{n} is the direction of the normal vector, ρ is the density, dA the control surface, and e is the total energy per unit mass [10].

The corresponding Navier-Stokes equations for a transient system are described by equations 2.5 to 2.7. These equations are used for simulating the radiator model [18].

$$\dot{m}_{in} = \dot{m}_{out} \quad (2.5)$$

where \dot{m} is the mass flow. The mass flow is constant across the component since no mass can disappear according to conservation laws. The total pressure at the in- and outlet are calculated according to:

$$P_{0_{out}}^1 = P_{0_{in}} - P_{loss}(T, \dot{m}) \quad (2.6)$$

where P_0 is the total pressure. The total pressure at the outlet is the total pressure at the inlet minus the pressure drop occurring across the component. The pressure drop is dependent on temperature and flow rate. The temperature difference across the radiator is calculated as:

$$T_{system} = \int \left(\left(\nabla \frac{k(T)}{\rho C_p(T)} \nabla T \right) - u \frac{\partial T}{\partial x} - \frac{1}{\dot{m} C_p(T)} \dot{q}_{Loss} \right) dt \quad (2.7)$$

where k is the conductivity, ρ is the density, C_p is the specific heat, u is the velocity and \dot{q}_{Loss} is the heat rejection. The first term in equation 2.7 represent the thermal diffusivity. Thermal diffusivity is a measure of how well a material is able to conduct thermal energy relative to its ability to store thermal energy [20]. The second term represents the effect of the momentum on the temperature gradient described in the conservation laws, and lastly the third term describes the temperature difference that originates from the coolant rejecting heat to the ambient air.

Heat rejection from the coolant

The working principle of the radiator model is to calculate how much energy is added to the ambient air. The energy that the air receives from the coolant must be equal to the energy that the coolant rejects. By solving for the Nusselt number (considering the air side), one can extract the heat transfer coefficient and the heat lost from the pipes. The Nusselt number is calculated as [9].

$$Nu = 0.023 Re(T, U)^{0.8} Pr^{0.33} \quad (2.8)$$

¹ $P_{total} = \frac{\rho u^2}{2} + P_{static}$

where Re is the Reynolds number and Pr is the Prandtl number. The Reynolds number is determined as: [10]

$$Re = \frac{\rho LV}{\mu} \quad (2.9)$$

where L is the characteristic length, V is the velocity of the fluid and μ is the dynamic viscosity. The airflow varies and depends on three main factors: the vehicle speed, the fan speed and the ambient temperature. By specifying these three parameters, one can extract the air mass flow. The Prandtl number is calculated as [10]:

$$Pr = \frac{\mu C_p}{k} \quad (2.10)$$

where C_p is the specific heat and k is the conductivity. All these three variables are temperature dependent.

Once all the variables for the Nusselt number are calculated, the heat transfer coefficient can be determined according to

$$h = \frac{Nuk}{L} \quad (2.11)$$

With the heat transfer coefficient known, the q_{loss} could be calculated according to equation 2.12

$$q_{Loss} = hA\Delta T \quad (2.12)$$

where h is the heat transfer coefficient, A is the area of the pipe and ΔT is the temperature difference in the coolant.

3

Method

3.1 Introduction

System-level simulations is very beneficial for industrial purposes. System simulations can capture the physical properties of multiple components and how they interact with each other. Testing different concepts by employing virtual prototypes and hence reducing cost, time-to-market, increasing quality and safety This project focused on developing modeling methodology for performing the so called 0D system simulations for the complete vehicle thermal management system.

1D-solvers can serve multiple purposes. It can be used to solve fluid simulations, map based approach for electric motors and simplified modeling of battery packs. Even though 1D-solvers are fast and efficient, it is possible to simplify the simulation environment even further. This is done by using a 0-D simulations. This simplification allows for faster simulations and improved optimization capabilities. MATLAB/Simulink enables the user to run 0-D simulations with information regarding different flow properties already summarized in nodes. The data originates from a multiphysics system simulation software named GT-SUITE. Since all the equations already are solved, the number of CPU hours decrease dramatically when simulating the same system in Simulink.

The thermal management system can be divided into four different subsystems: electric drive circuit, high voltage battery circuit, climate circuit and cooling pack see figure 3.1.

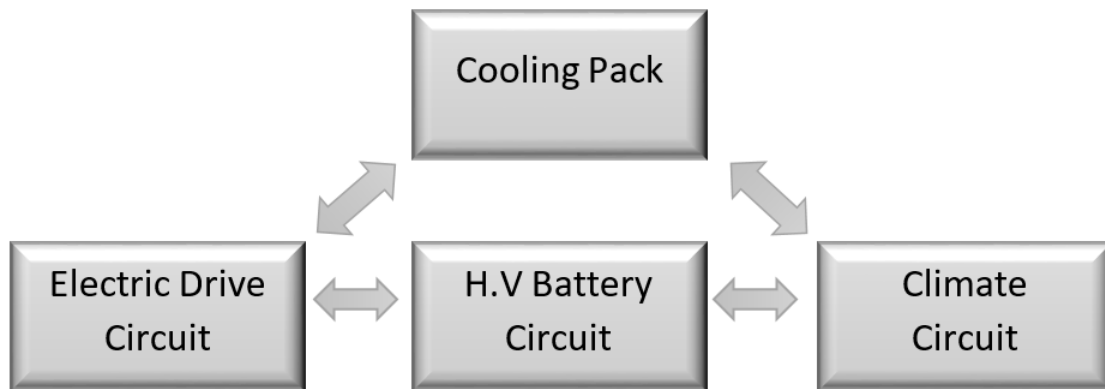


Figure 3.1: The three subsystems; Electric Drive Circuit, HV Battery Circuit, Climate Circuit and Cooling Pack

As seen in figure 3.1, the three circuits can interchange coolant with each other by changing the valve openings. This is crucial to maintain a proper working temperatures for the internal components and achieve high energy efficiency.

3.2 BEV components

This section briefly presents information regarding the working principle of the components within the four subsystems and their impact from thermal management point of view. Some of the components are seen in figure 3.2

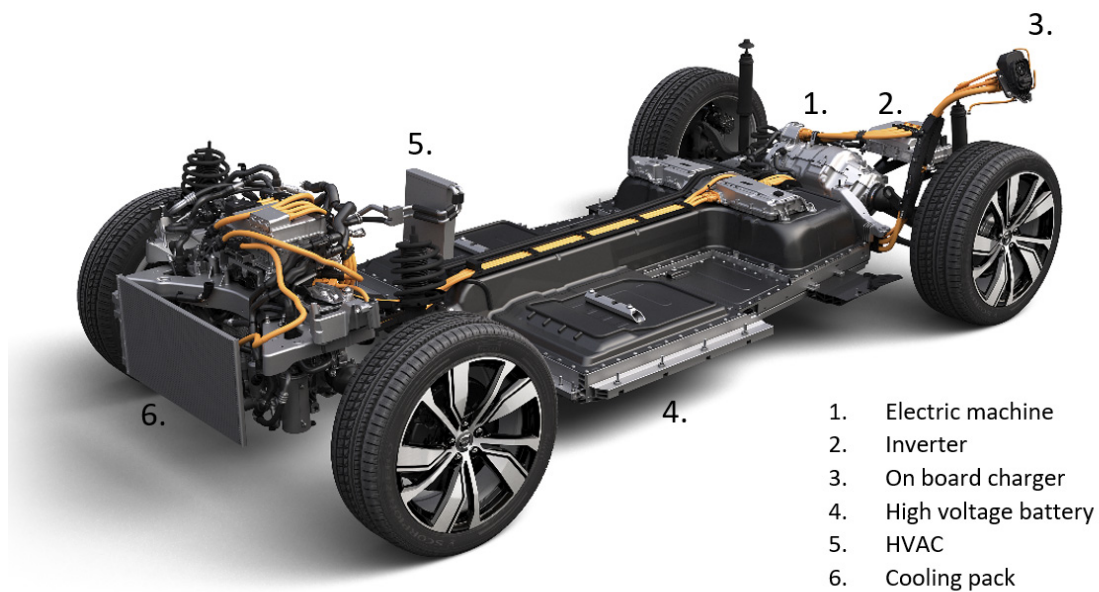


Figure 3.2: BEV components

Electric Machines

An electric machine propels the vehicle by converting electrical energy from the battery to mechanical energy. The maximum energy efficiency of an electric motor is normally around 75% [6]. Since a motor is a component with high energy demand and relatively low energy efficiency, some of the energy will be converted into heat. High temperatures result in high copper resistance in the windings and demagnetizing of the permanent magnets. This leads to lower machine torque and increases the winding failure rate. "It is a rule of thumb that 10°C temperature increase halves the life expectancy of an electric machines" [13]. The temperature for an electric machine should not exceed 100°C [16].

Inverters

The inverters are assigned to regulate the speed and torque from the electric machines. They do this by converting DC (direct current) from the batteries into the 3-phase AC (alternating current). When the vehicle is in energy regenerating mode (braking), the inverter is tasked to do the opposite conversion, from 3-phase AC to DC. This enables the battery to charge during braking. For a motor to function, an inverter has to be installed up-streams of the electric machine. In the modeled system, there are two inverters: IEMF and IEMR (Inverter Electric Module Front/Rear). The temperature of an inverter should not exceed 80°C [16].

On Board Charger

The OBC (On-Board Charger) is connected to an external power source during charging. A major benefit of an OBC is that it allows for different power inputs and phases. The car can be charged with everything in between single-phase 1.9 kW to 3 phase 20 kW. The efficiency of an OBC varies but can reach up to 90 %. The higher the efficiency, the lower the losses and thereby the requirement for thermal management. If the efficiency is reduced, it will require some heat sink which is unfavorable considering both the limited space and increase in weight [3].

Vehicle control unit

The Vehicle control unit (VCU) is a low-voltage control module in charge of almost all processes relating to the functional aspects of a BEV. The VCU uses various driver inputs and estimates a torque value needed to get received by the inverter. The torque value is proportionate to the accelerator and brake pedal positions and the gearbox setting. This is adjusted via any other vehicle torque demands, such as the Electronic stability Control System (ECS).

High voltage battery

A HV battery is a battery pack that consists dozens of battery cells. Each cell comprises two electrodes called anode and cathode. These two are merged into an electrolyte and divided by a separator. The electrolyte carries both positively and negatively charged ions. Electrons are unable to travel through the separator and

are therefore forced to travel through a load. This movement of electrons is powering the device [15]. Lithium-ion batteries are currently the most attractive option due to their high energy/power density. The energy density within a lithium-ion battery is generally around 50-200 Wh/kg. The thermal management of batteries is crucial since the preferred temperature range is relatively narrow. The temperature within the battery should be around 0-45°C. The ideal temperature is 25°C [14].

Chiller

To dissipate heat through heat exchangers, there needs to be a hot and a cold medium. When the ambient temperature exceeds the battery operating temperature range, an additional cooling source is required. For that purpose a chiller is connected both to the climate and battery circuit through a refrigerant loop. This allows for further temperature reduction of the coolant [17] even though the ambient temperature is high.

HVAC

The primary purpose of an HVAC (Heating Ventilation and Air-Conditioning) is to regulate the temperature inside the vehicle cabin. Depending on the ambient conditions, the heating and cooling demand can either be collected from external sources, such as chillers and PTC (Positive Temperature Coefficient) or directing the coolant with valve openings. It is favorable to avoid using external sources to reduce the energy consumption[11].

HVCH

High Voltage Coolant Heater (HVCH) is placed in BEVs to warm up both cabin and high voltage battery in cold ambient temperatures. It converts DC electric power into heat without loss [19]. This component is essential to increase the BEVs range and extend the battery cell when the ambient temperature is low.

3.3 Simulink

Simulink is a powerful tool that allows for model-based design in a block diagram environment. The tool was chosen for this project due to its capabilities of handling simulations on a system level. Simulink is integrated into MATLAB, which enables the user to incorporate MATLAB for post-processing purposes and further analysis [21]. While there is a predefined library within Simulink with various components in different physical domains, it was not used in this study. Instead, a component-based library was constructed with GT-SUITE with most of the data originating from GT-SUITE. A component-based library entails that the models within the system are based on specific components. This implies that as long as the components within the system remains unchanged the extracted model can be used for different types of analysis in different layouts.

Simulink uses a solving procedure seen in figure 3.3.

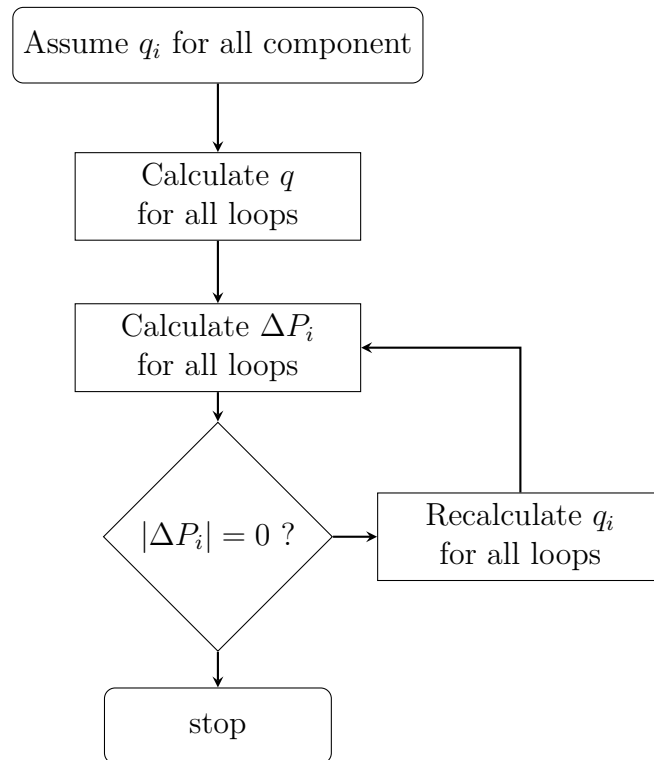


Figure 3.3: Coolant flow rate calculation flow chart

By using equation 2.1, a numerical process can be carried out to find the pressure drop for the components. The solving procedure assumes a mass flow rate for each of the components, estimates the mass flow rate in each branch from the total loop flow rate, and finally calculates the loop pressure drops. If the absolute value of these pressure drops are not close to zero with sufficiently small error, repeat the iteration on the loop flow rates until they are all zero.

3.4 Data acquisition

To understand how all the components within the system behave under various conditions, the system had to be simulated under various conditions. The three parameters that changed during this project were temperature, pump speed and valve positions. Seven different ambient temperatures were considered: -20, 0, 15, 30, 40, and 70°C. The pump speeds were varied 16%-100% of its maximum capacity. Six different valve arrangements were to be simulated to extract the profiles for the components. The total number of simulations required to build this simulation network under these conditions are 252. See figure 3.4 for graphical a representation.

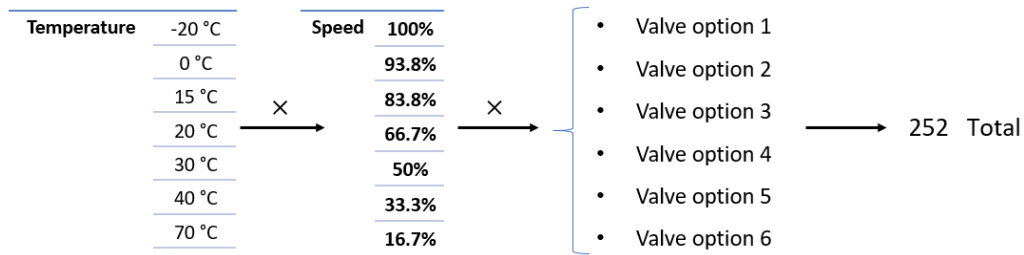


Figure 3.4: Simulations required

The state of the simulation was set to a steady-state and total time to 300 s. The results for the components were compiled in a *.txt* file.

3.5 Regression

The *.txt* was processed through the in-house script which delivered an excel file. The excel file contained all the results and made it possible to link the pressure drops for the various components. By doing so, one can extract the pressure drops between the components, i.e., the pipes. Once the pressure drop for the pipes was captured, the results were imported into MATLAB to perform the regression. Regression is a statistical method where the goal is to create a function which best match the observed data.

To process the data in Simulink, the simulation block called “n-D Lookup Table” was used. The dimension “n” is set after the number of dependent variables. For example, to calculate the pressure drop across a component (e.g a pipe), the dependent variables are temperature and flow rate. This implies, if the temperature is kept constant, a specific mass flow rate corresponds to a specific pressure drop, see figure 3.5.

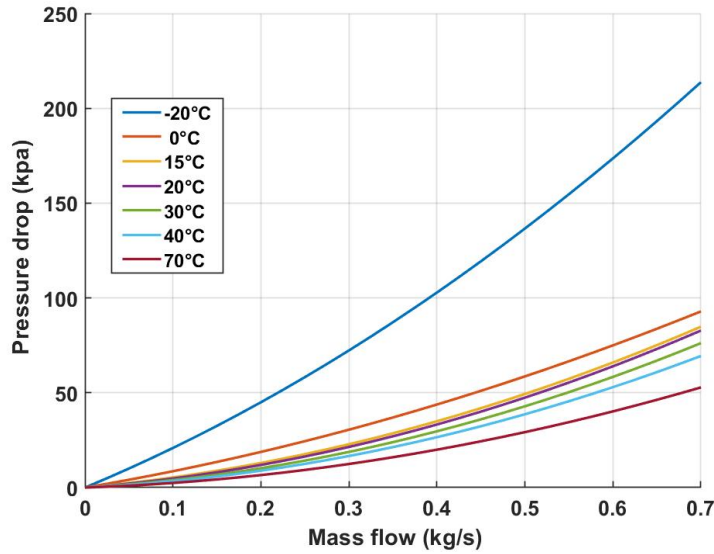


Figure 3.5: Pressure drops versus mass flow rate in a pipe under various ambient temperatures

This interconnection was used in the regression for the components. The regression in MATLAB was required for several reasons. First, regression is a viable option to expand the existing data range. Regression enables the model to handle scenarios that are not simulated in GT-SUITE, see an example in figure 3.6 where the range of the mass flow rates and pressure drops is increased to get an estimate of how the properties progressed. Secondly, Simulink can only perform a linear interpolation which is not as accurate as 2nd- or 3rd-degree order regression that can be performed in the MATLAB script. To mitigate the regression in Simulink, the pressure drops across a component had to be matched to a standard mass flow rate determined in MATLAB.

A second-order polynomial function (without a constant) was used to perform the regression for the pressure drop calculation based on the mass flow rate and temperature, see figure 3.6a. To extract the resistance, a third-order polynomial function was utilized, see figure 3.6b. The regression process is done by the in-house function called *Regression.m* which has the option to change the order of the polynomial function, or include additional elements to the dataset delivered by the regression. It is worth noting that the same settings in the regression function are not feasible for all the components. Depending on the component and boundary conditions, these settings had to be altered. It was observed that if the degree of the polynomial function was odd, it was more likely to perform a successful regression due to the characteristics of the data.

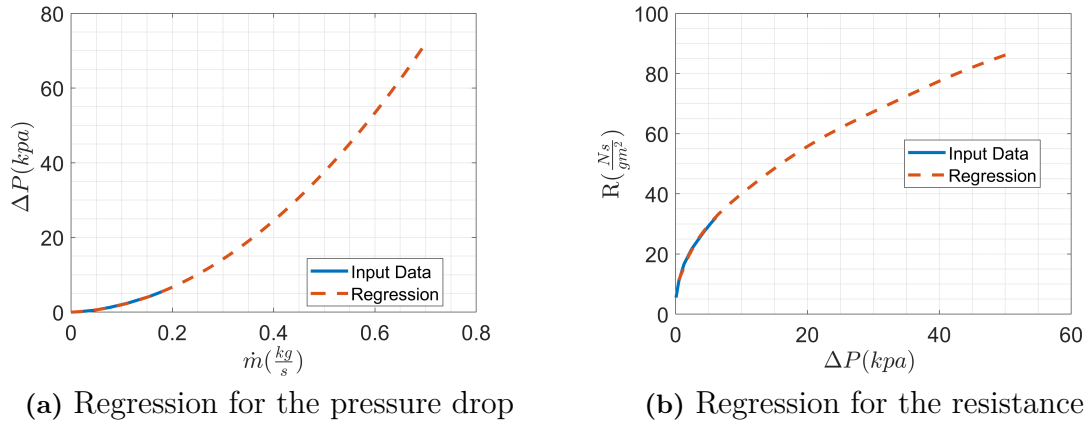


Figure 3.6: Regression for a pipe

Some components have a higher constraint on accuracy than others. The pump in a cooling the circuit is one of these components because the pump determines the flow rate. The flow rate is a dependent variable for the pressure drop calculation for all the internal components within the circuit. The regression for the pump, unlike the other components, is based on data provided by the supplier and not the GT-SUITE results. The supplier data contained information regarding flow properties such as pressure rise and flow rate under various pump speeds and temperatures. The regression for the pump was conducted in two steps. The objective of the first step was to perform the pressure drop regression to a specific predetermined mass flow rate interval (just like the other components). A third-order polynomial function was used to perform this regression, see figure 3.7a. The goal of the second step was to perform the regression for the resistance to a specific predetermined pressure drop interval. Just like in the first regression, a third-order polynomial function was used to fit the resistance to the new pressure range, see figure 3.7b. The new pressure and mass flow range was specified for two reasons. The first reason was that the data needs to be compiled in look-up tables where one needs to specify a certain data range for these two properties. Therefore, it was beneficial to perform the regression to the same data range to avoid having several data ranges for the different components. The second reason was to mitigate the regression in Simulink.

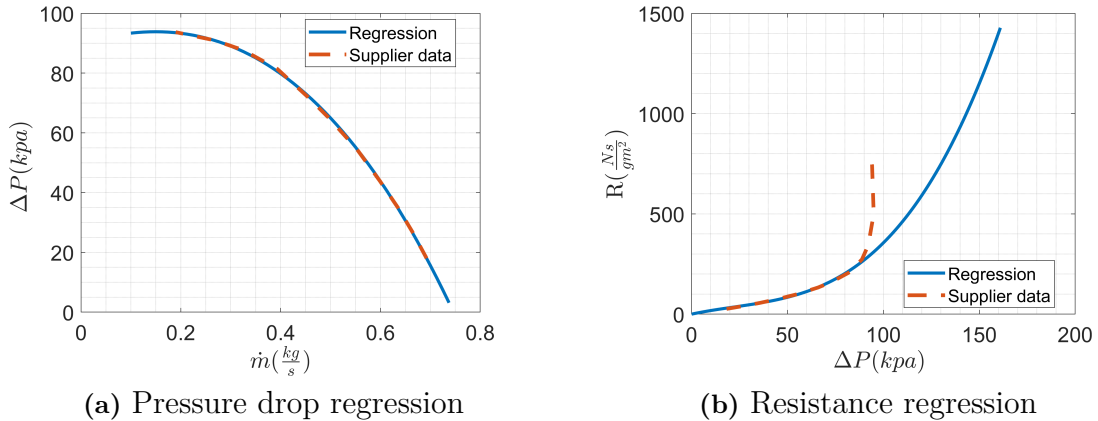


Figure 3.7: Regression for the pump

As seen in figure 3.7b the regression does not follow the sudden increase in resistance observed in the supplier data. This increase occurs when the mass flow is approaching 0 and is referred to as drooping. As seen in figure 3.7a, the head pressure of the pump can result in many different flow rates. This causes the pump to oscillate since there are several operating points to cover. This behaviour is undesired since it is unstable and coupled with low efficiency [26].

To enable the pump to have a linear increase in its speed and operate between the specific speed ranges that the supplier provided, this increase had to be disregarded in the regression. For example, a pump speed at 80% operating at 20 degrees corresponds to a pressure rise of 102 kPa. A pump that is operating at 100% at the same temperature results in a higher pressure difference, 143.9 kPa. If the sudden increase were included in the regression for the lower speed, the resistance for a pump speed of 90% would result in unreasonably high resistances. This problem arises since Simulink performs linear interpolations between two data points. There are three different pumps in the system, and the regression for all of them is built using the described principle.

3. Method

All the components in the library except the radiator model are based on lookup tables. Seen in the figure 3.8, all the components have the same in- and outputs, with the exception of the three pumps and the "pipe calculator". The input- and output ports Q, T, and P represent the flow rate, temperature, and total pressure, respectively. The flow rate will remain constant independently of the component. The temperature, however, changes depending on the component and the scenario. Components that have high energy consumption generate some heat due to inefficiencies. The components that will add heat to the coolant are the two inverters (IEMF & IEMR) and the two electric machines (ERAD & EFAD). The radiator, however, will reject heat from the coolant. All the other components are assumed to be adiabatic. All components in the circuit experience a pressure drop which implies that the total inlet pressure is not preserved across the component. An example of the signal change across the EFAD-component is illustrated in figure 3.9.

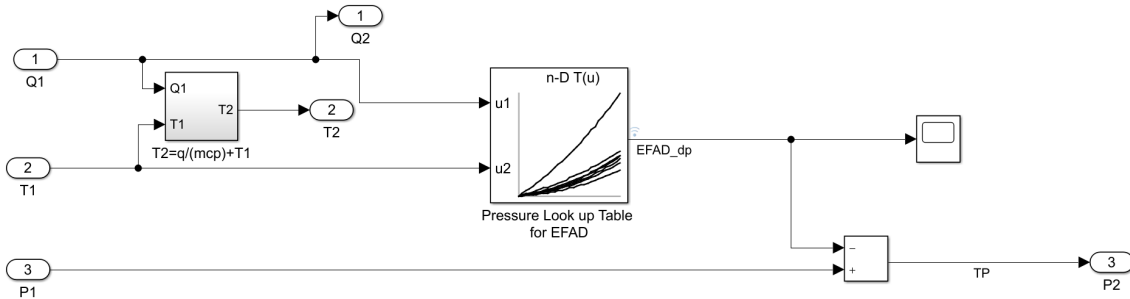


Figure 3.9: The component EFAD in the Simulink library.

To model the pressure drop across a given component, a lookup table is used. By specifying the inlet temperature and flow rate, one can determine the pressure drop. This pressure drop is then subtracted from the total inlet pressure to calculate the total outlet pressure. The temperature increase is calculated as:

$$q_{Loss} = \dot{m}C_p\Delta T \quad (3.1)$$

Here q_{Loss} is the heat loss, \dot{m} is the coolant mass flow, C_p is the specific heat capacity and ΔT is the temperature difference across the component. Heat loss is an input variable that varies over time, and its value depends on the specific scenario. Scenarios describe common driving patterns were used to model the thermal aspect of the system. This will be explained in more detail in chapter 3.8. By changing the scenario and implementing the new heat loss for the specific component, one can model multiple scenarios. Initially, the heat loss was set to 0 to lower the complexity and achieve accurate flows. With the heat loss known, one can determine the output temperature T_2 . The pressure drop and temperature increase/decrease are calculated with the same principle for all the other components. The library consists of two pipe-blocks. One of them contains information regarding the pressure drop, while the other carries the resistance profile. These are denoted "Pipes" and "Pipe calculator" in figure 3.6. The "Pipe calculator" was used to determine the flow rate in parallel connections while the "Pipes" calculated the pressure drop. The

pipe blocks were masked to avoid having multiple pipes in the library. The mask option allows the user to specify which pipe should be included when importing the "pipes" block.

There are two thermal models in the system, battery and radiator. The radiator model denoted RAD ED in the library has gradually increased in complexity during this project. Initially, it was modeled as the rest of the components with a single pressure drop across its boundaries. Once the heat was added to the electric components, the model was customized in order to be able to dissipate excess heat. More details how this was accomplished can be found in section 2.2. The thermal battery model was provided by another department at Volvo Cars.

3.7 Modeling in Simulink

The components in the library can be aligned with one another in different ways, either in series or in parallel. To successfully design a network containing both these alignments, the system had to be simplified initially. The system started by having a single pipe aligned in series with a pump. Once the simulation was proven to be stable and accurate, an additional component was added in series and then later a parallel connection. To simulate the pressure drop in a series connection, one directs the total flow through both components and adds up the corresponding pressure drops, see figure 3.10. This is not the case for a parallel connection. The flow rate is split into two branches, and the amount of flow in each branch is dependent on the corresponding resistance (like an electric circuit). To simulate this in Simulink, one calculates the pressure drop in the branch and the corresponding resistance. With these two determined, one can calculate the flow rate.

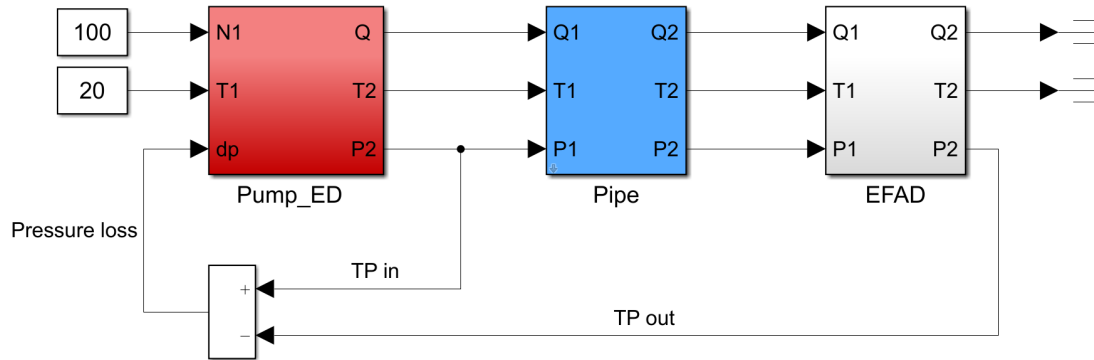


Figure 3.10: Pressure drop for components that are connected in series

During the modeling phase it became clear that the regression done automatically in Simulink did not possess the same accuracy as the one that was performed in the MATLAB script. Simulations became unstable when the flow was split into several branches. This issue was solved using several remedies. First, the range of the specified mass flow and pressure drop was increased in the MATLAB script. This adjustment ensured that the extrapolation was not done in Simulink. Two other blocks that were proven to be necessary were the moving averaging block and the saturation block. The moving average blocks allow the simulation to oscillate over certain values and then find the average. The saturation block was used to guide different properties of the flow during low pump speeds and temperatures.

Once the simple layouts were set properly, the real layout was implemented and modeled. See the three subsystems in figure 3.11.

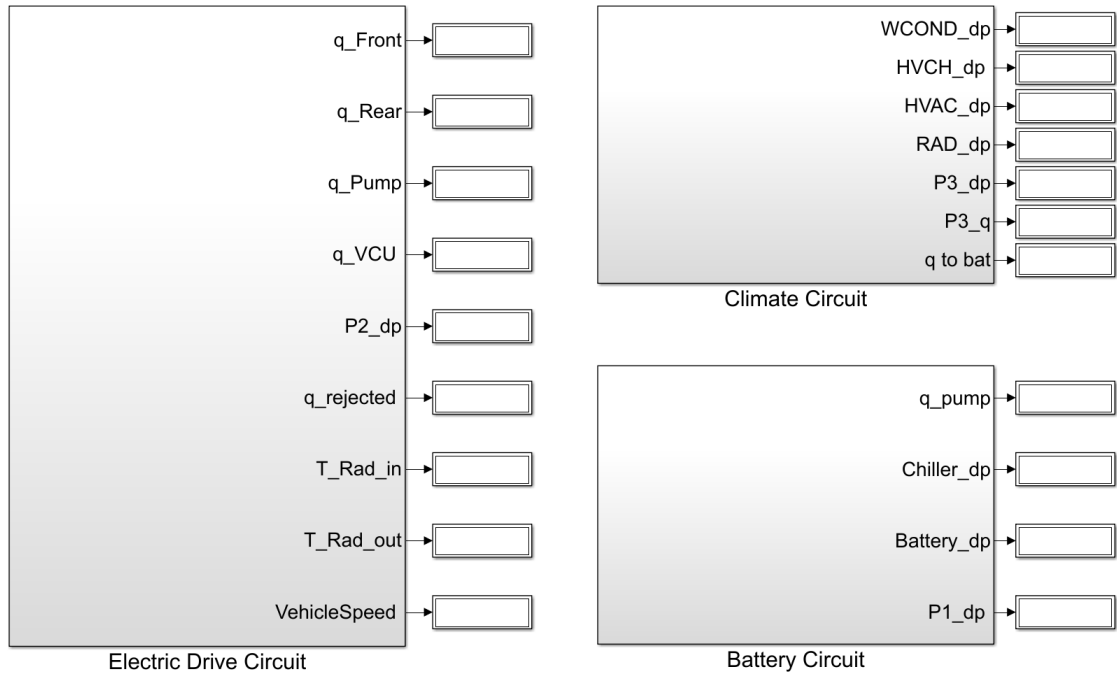


Figure 3.11: The three subsystems: Electric Drive, Battery and Climate Circuit

These three circuits can either work separately or interchange fluid depending on the valve openings in the subsystems. The valves in the circuits are all 2-way valves and are controlled with a simple switch. The switch is controlled by changing the input from a 1 to a 0 and vice versa. This possibility of directing the flow in different directions and the possibility to isolate specific circuits is highly valued when one wants to study a specific subsystem in more detail. The entire system, including the valve positions, is controlled by an input file from MATLAB, see the MATLAB code provided in Appendix A.1. In the input file one can specify the information regarding pressure profiles, C_p -values, radiator variables, state of the simulation, ambient temperatures, etc. As seen in MATLAB code, the state of the simulation can be specified by changing 1 to 0 and vice versa. This possibility is desired to increase the system's flexibility and was achieved by constructing two branches side by side. Depending on the value of the switch, only one of the branches can be active, see figure 3.12.

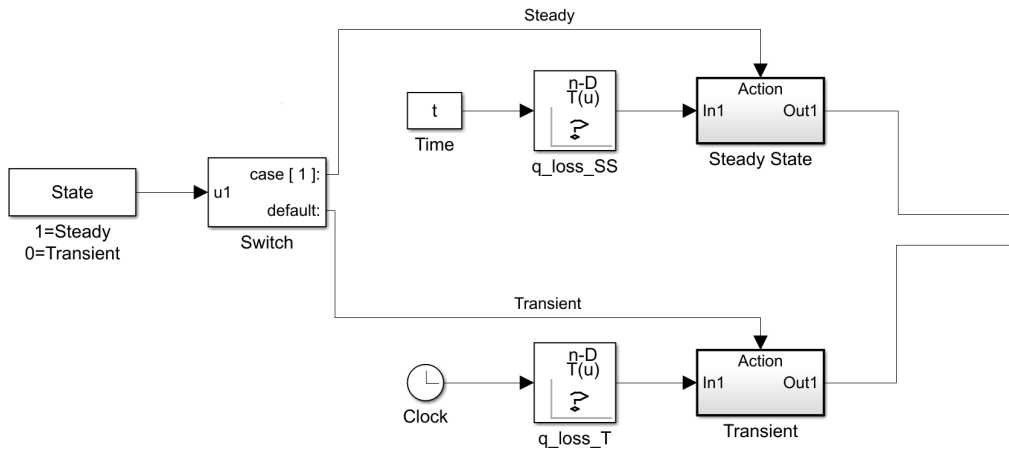


Figure 3.12: State switch in ERAD

For the steady-state case, one needs to specify the time of interest in the scenario.

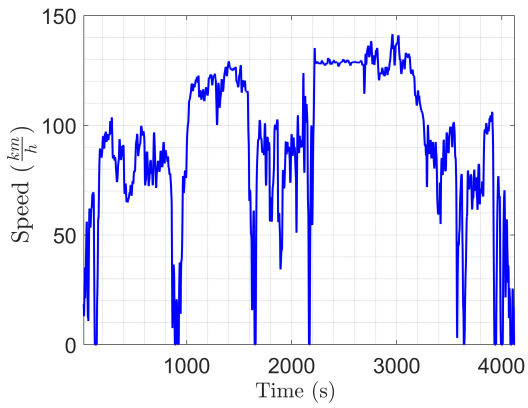
3.8 Modeling scenarios

Three different scenarios were modeled in this project. Two of the scenarios was modeled for two temperatures, see 3.1. The scenarios were simulated to validate the accuracy and test the flexibility of the cooling system. A scenario describes a particular driving cycle which drivers usually encounter. See the velocity profile in figure 3.13.

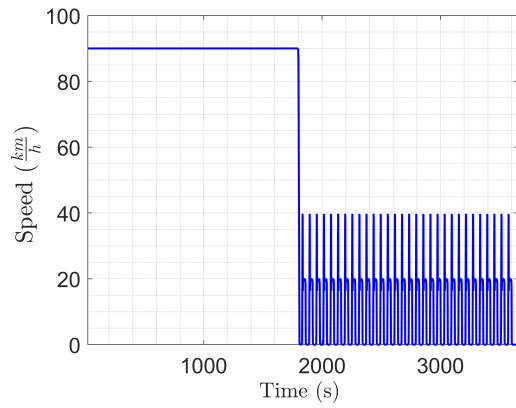
Table 3.1: Scenarios tested

Scenario:	Highway driving	City driving	WLTC
Temperatures:	15°C and 35°C	46°C	15°C and 35°C
Time:	4123s	3660s	3600s

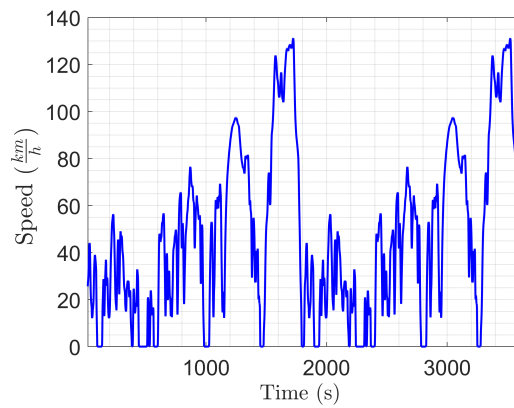
To model a specific scenario, one needs to obtain some time-dependent information about the specific components within the system. The variables used to simulate a scenario were the heat generated in the two electric machines and inverters, the vehicle velocity, and the battery current. If the power loss is established, one can determine the outlet temperature of the component, see how this is done in chapter 3.6 equation 3.1.



(a) Vehicle speed highway



(b) Vehicle speed city driving



(c) Vehicle speed WLTC

Figure 3.13: Vehicle speed for three different scenarios (highway driving, city driving and WLTC)

3.8.1 Highway driving at 35°C and 15°C

The velocity profile for the highway scenario is shown in figure 3.13a. There are several variables to study in the highway driving scenario at 35°C. The immense power requirement is reflected in the losses and thereby the temperature increase over the electrical machines. To avoid overheating the components, this additional heat needs to be rejected in the radiator. On the other hand, a high vehicle velocity results in more convection and more heat transfer to the surrounding air through the cooling pack. It should be noted that the ambient temperature of 35°C is not low enough to activate passive cooling for the battery. It can only lower the temperature in the electric components since they have a higher working temperature. To enable passive cooling, another scenario was conducted with a lower ambient temperature of 15°C. Since the temperature is well below the operating range of the battery, passive battery cooling is a valid option. Passive cooling is enabled by connecting the electric drive circuit to the HV battery circuit. This implies that the coolant will be heated up in the battery and the electric machines before it passes through the cooling pack.

3.8.2 City Driving at 46°C

Another common driving scenario is the city driving at high ambient temperatures. This scenario consists of a constant driving speed followed by several starts and stops. The constant velocity in the beginning is included to stabilize the system before the fluctuating velocity profile begins, see figure 3.13b. The fluctuating velocity represents a queue (vehicles queuing in a line). Due to the high ambient temperature and low speeds, the heat rejection in the cooling pack will be limited.

3.8.3 WLTC at 35°C and 15°C

The WLTC (Worldwide Harmonized Light-Duty Vehicles Test Procedure) cycle is based upon 765000 km of driving in various locations worldwide. It is designed to be applicable to many regions and is a popular driving scenario to simulate since it offers a harmonized driving cycle. A harmonized test is developed by organizations to ensure that the products are tested to satisfy national standards.

It combines different driving conditions for short trips, and the goal is to make it as representative of a regular short trip as possible[25]. As seen in the velocity profile, parts of the cycle contain high velocities while others have lower velocities.

4

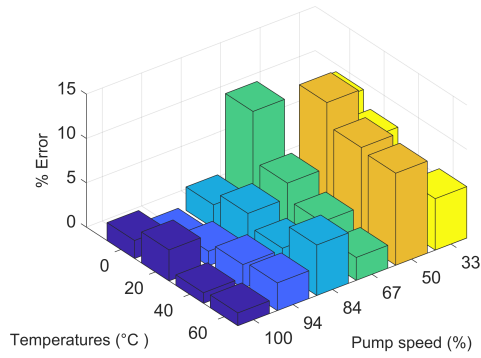
Validation

This chapter will present results and analysis regarding the cooling system modeled in Simulink. The credibility of the Simulink model will be based on data from the supplier and the results seen in GT-SUITE. The properties of interest when doing the modeling in Simulink are temperature, pressure and flow rate. The accuracy of these three properties determines how well the model is performing.

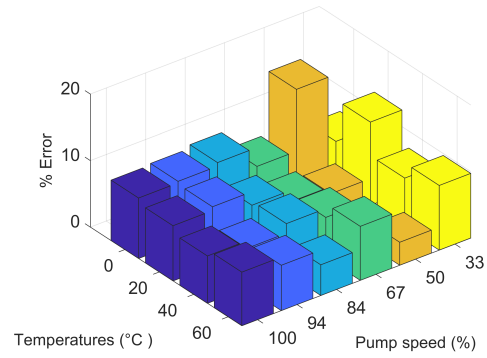
4.1 Steady-state scenario

An error analysis for the three subsystems was conducted. This is required in order to reach an estimate of confidence for the system. Without an uncertainty estimate, it is impossible to answer how well the model actually agree with the sources it is validated against [12]. As mentioned previously, the pump is a component of high importance. The properties of the pump should reflect the properties of the system. According to Kirchhoff's laws, the total flow rate and pressure drop in the system should be equal to the total flow rate and pressure increase in the pump, see section 2.1. The pump sets the flow rate in the system. This is accomplished by matching the pressure rise in the pump to the pressure drop in the circuit. Since there is a minor error for the pressure drop calculation for each component, the pressure drop seen in Simulink will not be similar to the one in GT-SUITE. This reflects in a miss-matched pressure rise in the pump and mass flow. In figure 4.1- 4.3 the three pumps for the three subsystems are presented in the form of an error analysis (with the supplier data as validation). The figures display the error in mass flow and pressure rise.

4. Validation

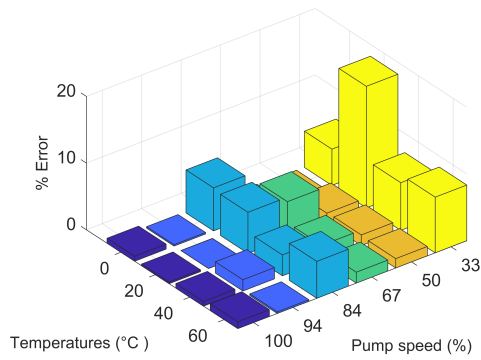


(a) Error in pressure rise

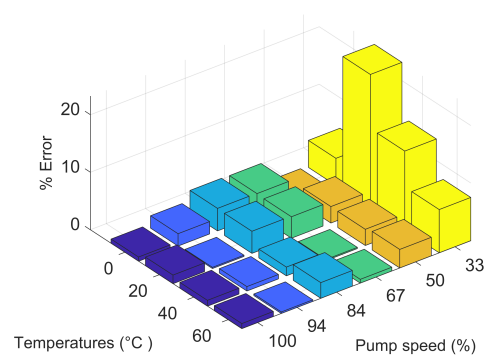


(b) Error in mass flow

Figure 4.1: Results for the pump inside the HV battery circuit

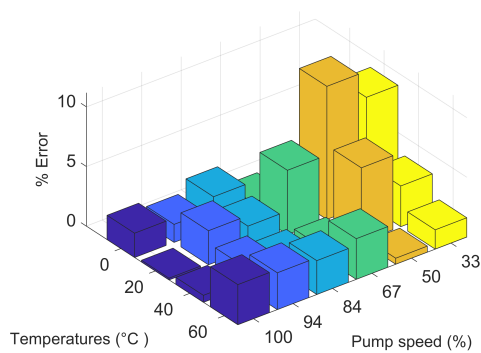


(a) Error in pressure rise

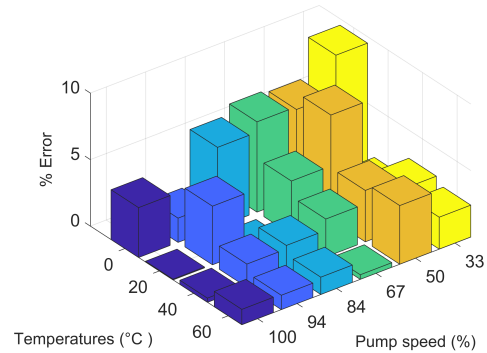


(b) Error in mass flow

Figure 4.2: Results for the pump inside the electric drive circuit



(a) Error in pressure rise



(b) Error in mass flow

Figure 4.3: Results for the pump inside the climate circuit

An acceptable error range for the three pumps was set to $<10\%$. This range was reasonable due to the difficulties found during the regression for the pump. To make the pump work in between the speeds that the supplier provided, some of the data had to be disregarded to make the regression feasible, see section 3.5. The error for the pumps is generally low. However, the error increases when the temperature and pump speed decrease. This is due to the reduction in absolute mass flow in the system. Once the absolute value of pressure and mass flow, decrease the absolute difference in these two properties becomes small and difficult to match in the regression. It is worth noting that the supplier also struggle to capture the pressure rise accurately for low pump speed. It is challenging to reduce the error in the system when the dispensing volume is varying and needs to be delivered by the same system [24]. To get the uncertainty estimate for the pump models, the errors for the pumps were averaged. The absolute error for the battery pump, electric drive pump and climate pump are 4.92%, 2.76% and 2.53%, respectively. Since the error is below the 5%, the fidelity of the pumps is considered to be high.

The complete system is validated against the results from GT-SUITE. The mass flow accuracy flowing through the components is of high importance during the pressure drop calculation. Since the pump is delivering the mass flow, the error in the pump will be reflected in the error for the components, see figure 4.4. The error for the pressure drop is displayed for each component within the three subsystems.

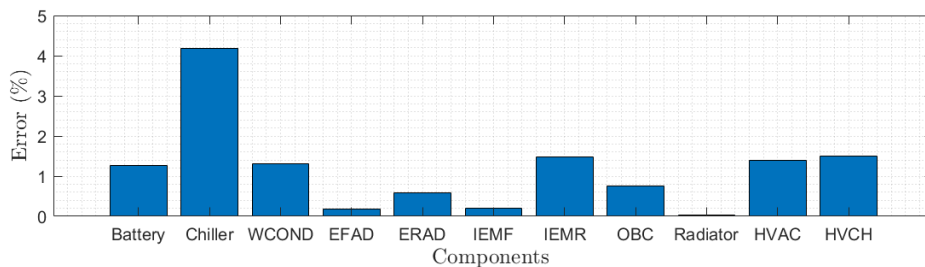


Figure 4.4: Error comparison for all components at the ambient temperature of 20°C at 100% pump speed.

See how the error changes for 0°C and 40°C in figure A.2 in Appendix. As can be seen in the figure, the regression for the components are done with high accuracy. One can therefore conclude that the only "weak spot" in the model is the pump. Like the pump, the acceptable error limit is $<10\%$ which all the components are well below.

4.2 Transient scenarios

This section presents the results from the scenarios described in chapter 3.8. All the scenarios use GT-SUITE as validation. Since no thermal model was created for the climate circuit, it will be disregarded in this section. Both the HV battery circuit and the electric drive circuits contain thermal models and will be investigated further. Depending on the ambient temperature, these two circuits can either be coupled or isolated from each other. When they are coupled, passive cooling is enabled.

4.2.1 Highway Driving at 35°C

The electric drive circuit is the only subsystem that is investigated during the highway driving scenario at the ambient temperature 35°C. The objective in this scenario is to match the temperature difference in the electric machines, inverters and radiator that take place in GT-SUITE. In this manner the optimal working temperature for the systems is ensured. The components that are of high importance in this scenario are the components that generate and dissipate heat. The components that generate most heat are the electric machines together with their corresponding inverters. To match the heat transfer taking place in GT-SUITE simulations, the flow rate across the electric machines needs to be adequately matched. The error for the mass flow rate over the front and the rear machines can be seen in figure 4.5.

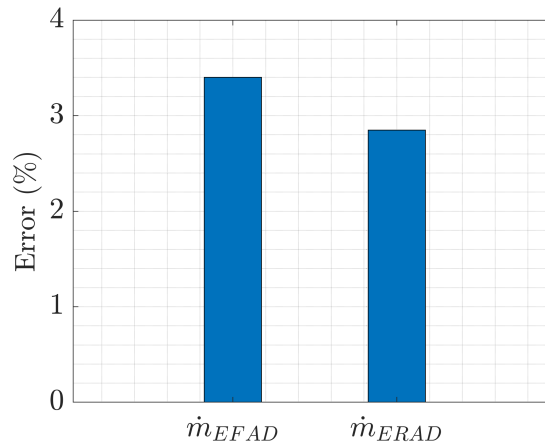
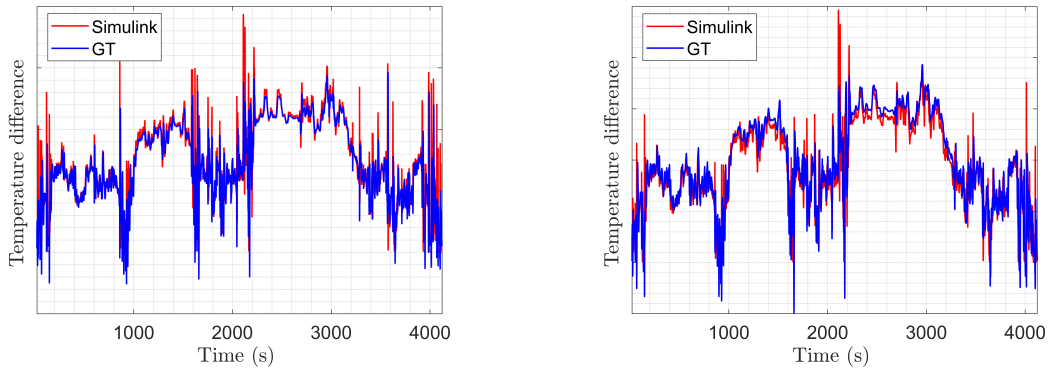


Figure 4.5: Error for the mass flow across the two electric machines

The error for the mass flow in the two branches is within 5% error during the entire cycle. The temperature difference across the electrical machines is seen in figure 4.6b and 4.6a.



(a) Temperature difference over the front electric machine

(b) Temperature difference over the rear electric machine

Figure 4.6: Temperature difference in the front and rear electric machines

it is observed in the two figures, the Simulink model matched the temperature difference from GT during the entire cycle within 5% error. See the temperature difference over the two inverters in figure A.3 in Appendix. The heat that is generated in the electrical machines and inverters is dissipated in the cooling pack. See the temperature profile over the radiator in figure 4.7.

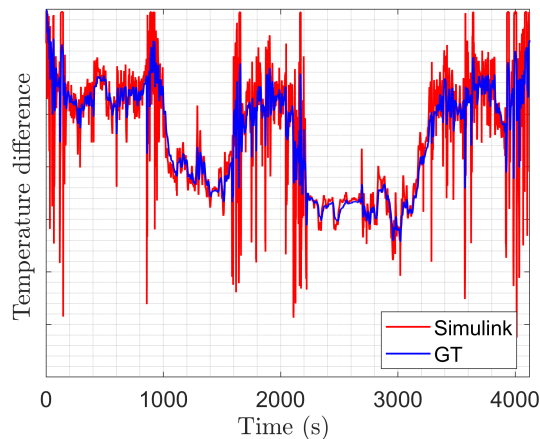


Figure 4.7: Temperature difference in the radiator

The trend from GT-SUITE simulations is followed during the entire cycle. However, the Simulink model exaggerated the peaks in temperature difference that occur in GT-SUITE. The mass and the thermal inertia is neglected in the Simulink model. This implies that the changes that occur in the loss will be instantaneous. These changes are not feasible in GT-SUITE where the mass is included. In a CFD simulations, the solver accounts for previous time steps and ensures that the changes are feasible. The high accuracy in the mass flow and temperature will be reflected in the total heat transfer in the radiator. See Appendix A.4 for the heat transfer

predictions being within 5% margin.

4.2.2 Highway Driving at 15°C with passive cooling

The same highway driving cycle is considered together with the losses that occur in the electrical components. The differences are that the ambient temperature is decreased, and the HV battery circuit and the electric drive circuit are connected. The objective in this scenario is again to obtain the correct working temperature for the internal components. This is achieved by matching the mass flow and temperature difference (Obtained from GT-SUITE simulations) across the components that generate and dissipate heat. The error in the mass flow rates flowing through the battery and radiator are shown in figure 4.8.

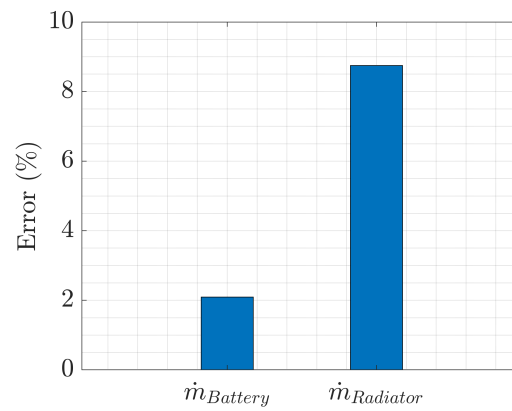


Figure 4.8: Error for the mass flow across the battery and radiator

The mass flow rate error in the radiator is 9 % while the battery remains below 3 %. These results are reflected in the heat transfer, see figure 4.9.

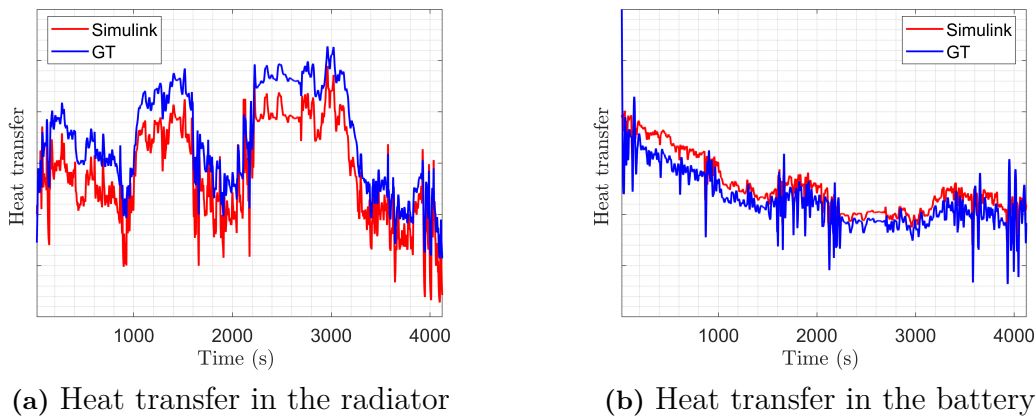


Figure 4.9: Heat transfer in the radiator and battery

The error for the heat transfer in radiator and battery is approaching 19.65% and

14.04% respectively.

4.2.3 WLTC at 35°C

Like in the highway scenario at 35°C, the electric drive circuit and the HV battery circuit are isolated. The average velocity and heat losses for the electrical components are 50% less compared to the highway scenario. This implies that less heat is generated in the electrical components. The error for the mass flow rates over front and rear machines is seen in figure 4.10

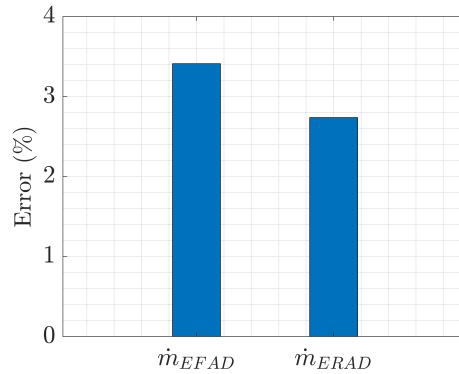
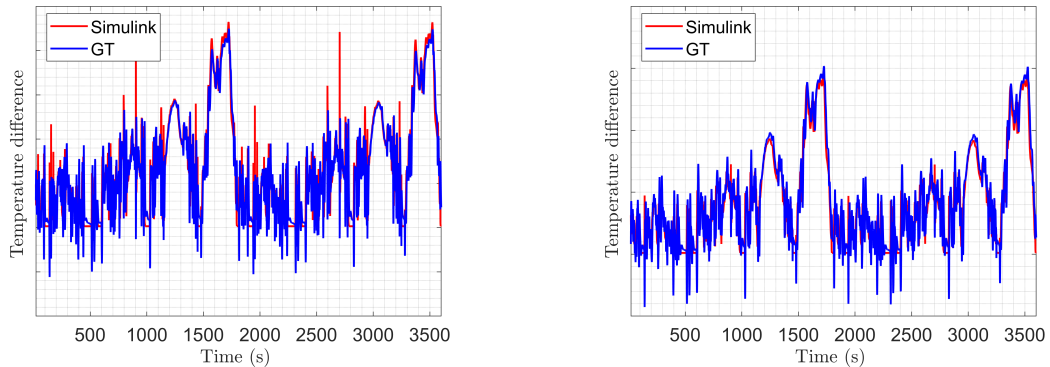


Figure 4.10: Error for the mass flow across the front and rear electric machines

The average error is below 5% for the front and rear electric machines. This result implies that the pressure drop is captured accurately for both branches. The temperature difference over the two electric machines can be seen in figure 4.11



(a) Temperature difference over the front electrical machine

(b) Temperature difference over the rear electrical machine

Figure 4.11: Temperature difference over the electric machines

The temperature difference in the electric machines for Simulink and GT-SUITE is similar. The heat that is generated in the machines is dissipated through the radiator. See the heat transfer in the radiator in figure 4.12.

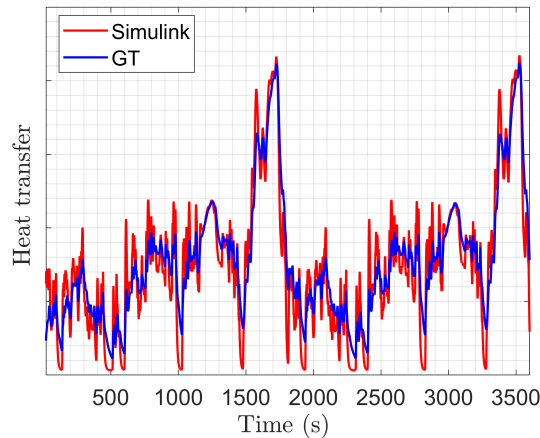
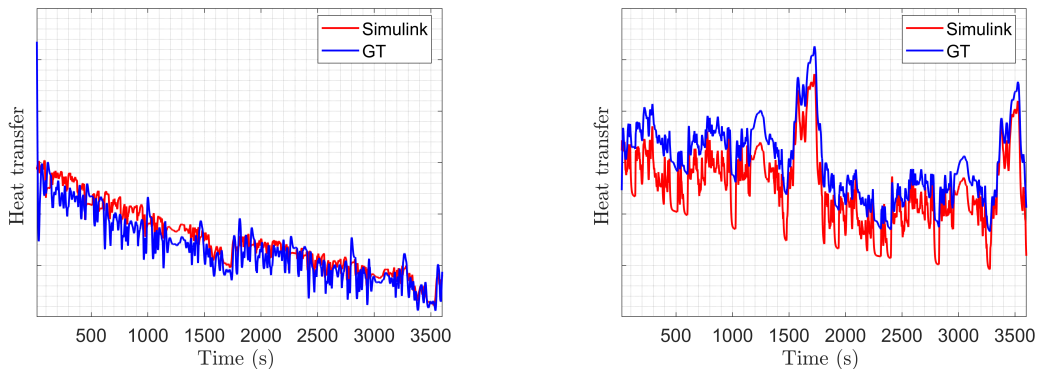


Figure 4.12: Heat transfer in the radiator

Just like the HW scenario at 35°C the heat transfer in the radiator is similar to the one seen in GT.

4.2.4 WLTC at 15°C with passive cooling

If the same driving scenario is investigated at the lower ambient temperature 15°C, one can enable passive cooling. The heat transfer to the battery and the coolant and the heat dissipated in the radiator are shown in figure 4.13.



(a) Heat added to the coolant in the battery

(b) Heat dissipated in the radiator

Figure 4.13: Heat rejected from the battery to the coolant

Similarly to the HW at 15°C, Simulink results follow the trend regarding the heat dissipated in radiator. However, the model underestimate the amount of heat rejected. This is due to the error in coolant flow rate flowing through the radiator, which is approaching 10 %. See the error in mass flow and battery in figure A.5 in Appendix.

4.2.5 City Driving at 46°C

The city driving scenario is challenging in terms of energy efficiency. The scenario contains several starts and stops at the high ambient temperature 46°C. The fluctuating velocity profile and the instantaneous losses that entails is challenging for the Simulink model to capture with the same precision as the previous scenarios. Since the ambient temperature is high, the two circuits need to be separated from each other. The battery is cooled with a chiller, and the radiator cools the electric components. The dissipation in the radiator is limited due to the high temperature and low air flow velocity. The error for the mass flow in the front and rear electric machines can be seen in figure 4.14.

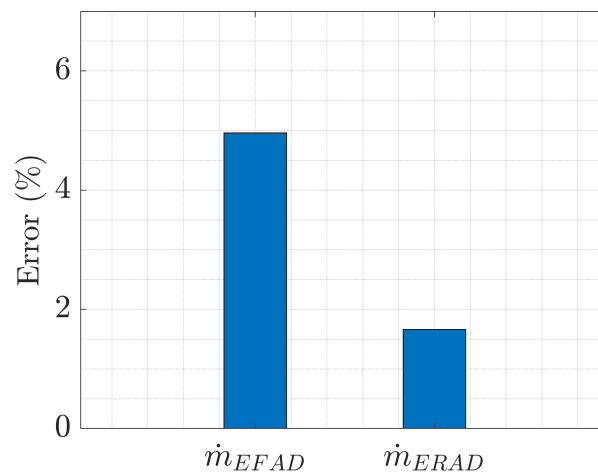
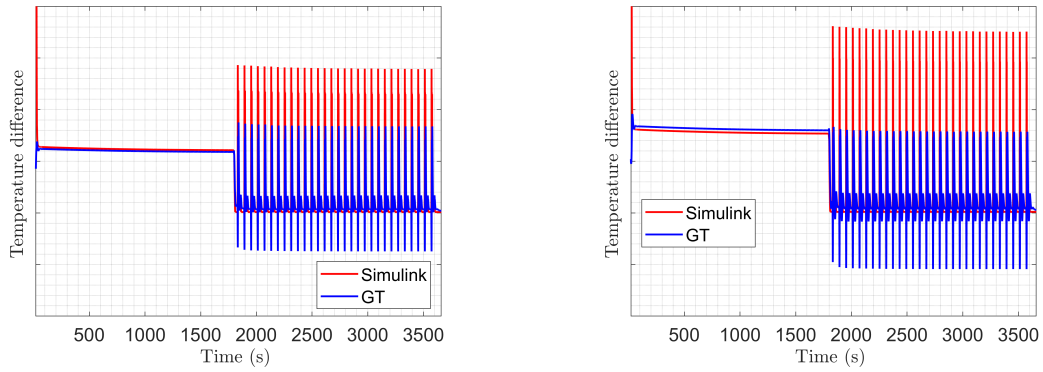


Figure 4.14: Mass flow error for front and rear electric machines

The temperature fluctuations in the system are too small to cause any oscillation problems for the mass flow. The temperature profiles over the electric machines are not captured with the same accuracy. As seen in figure 4.15, the temperature profile in Simulink is shifted upwards compared to GT-SUITE.



(a) Temperature difference over the front electrical machine

(b) Temperature difference over the rear electrical machine

Figure 4.15: Temperature difference over the two electrical machines

This shift occurs since the electric machines are considered massless in the Simulink model. GT-SUITE predicts a negative temperature difference in some time steps, implying that the machines are absorbing heat. Another thermal model for the electric machines has to be built to capture this temperature profile with higher accuracy. These models were built, but not included in the present results due to lack of time. Since the system is not reflecting GT-SUITE simulations to the same extent as the previous scenarios, the temperature profile over the radiator will not be captured with high accuracy, see figure

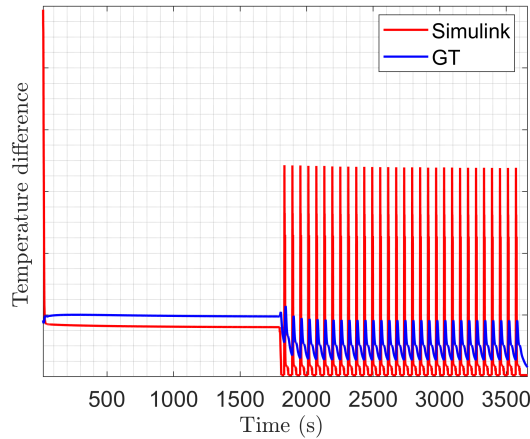


Figure 4.16: Temperature difference over the radiator

If the mass for the respective component are included these drastic changes can be mitigated.

4.3 Remarks from the validation phase

When studying the system from the perspective of the fluid flow, it was observed that the results for the flow pumps are of the highest importance for the entire system. In the least favorable scenario, the error for the pumps reach 20 % but was average below 5 %. Inaccurate predictions of the mass flow rate for the pump will affect the accuracy of all internal components. Therefore, it is crucial to study the total mass flow rate in the system before drawing any conclusion about the components affected by it.

The pump also had an impact for the scenarios that had passive cooling enabled. The error in mass flow for these simulations reached 9% which ultimately lead to a mismatched heat transfer rate in the battery and radiator.

Table 4.1: Simulation time comparison between GT-SUITE and Simulink

	GT-SUITE			Simulink		
	Time-step (s)	Simulation time (h:min:s)	Factor of real time	Time-step (s)	Simulation time (h:min:s)	Factor of real time
Highway 35°C	0.1	12:58:03	11.33	0.1	00:00:24	0.0058
Highway 15°C	0.1	04:01:07	3.52	0.01	00:04:12	0.0611
WLTC 35°C	0.1	07:11:06	7.19	0.1	00:00:24	0.0066
WLTC 15°C	0.1	03:34:06	3.58	0.01	00:03:27	0.0575
City cycle 46°C	0.1	05:28:52	5.39	0.1	00:00:23	0.0065

The Simulink model only requires a fraction of the simulation time compared to GT-SUITE. It can be seen in table 4.1 that the total simulation time increases once the temperature drops to 15°C. This increase is due to the reduction in time step which is lowered to 0.01 s compared to 0.1 s that is used in GT-SUITE. This change was required in order to simulate the thermal battery model, which was analyzed for the lower temperatures. Changing the sample size is a compromise between accuracy and simulation time.

5

Conclusion

Performing analysis in 0D compared to 1D offers many advantages. Since the Simulink model is easy to use and is considerably faster than GT-SUITE, it can be used in several areas. For example, it should be used during the early design phase to construct an optimized layout. It can also be used to isolate specific components and perform fast and efficient analysis.

The validation phase showed that modeling the pumps for the three subsystems (battery, electric drive and cabin) significantly affects the system. Pumps deliver flow rate to the system, which are dependent variable for all the internal components. Even though the delivered flow rate can contain some error, the error for the specific components is generally negligible. This implies that from the perspective of the fluid flow, the pump is the only component within the system that can be improved. It was observed that the absolute error in pressure rise for all three pumps increased once temperature and the pump speed decreased. This is because the total flow rate in the system was decreased, resulting in small absolute differences in pressure rises but significant errors during validation. To maintain a low error for these boundary conditions, the regression for the pumps needed to be performed with high accuracy. The component became a high-fidelity component but has potential to be improved for these more demanding scenarios. However, it should be noted that these conditions are difficult for the supplier to capture accurately as well.

The accuracy of the model was proven to be higher than expected, which can broaden the use of the model. If some of the fluctuations in temperature could be alleviated, the model can take GT-SUITE role as a source of validation. This will substantially reduce the simulation time and allow for more efficient optimization procedure during both physical and testing.

Bibliography

- [1] Titov, Eugene, et al. Matlab/simulink framework for modeling complex coolant flow configurations of advanced automotive thermal management systems. Vol. 1. No. NREL/CP-5400-65441. National Renewable Energy Lab.(NREL), Golden, CO (United States), 2016.
- [2] Kiss, Tibor, Jason Lustbader, and Daniel Leighton. Modeling of an electric vehicle thermal management system in MATLAB/Simulink. Vol. 1. No. NREL/CP-5400-63419. National Renewable Energy Lab.(NREL), Golden, CO (United States), 2015.
- [3] Electric vehicle (EV) on-board chargers
<https://www.avnet.com/wps/portal/abacus/solutions/markets/automotive-and-transportation/automotive/power-train-and-ev-hc-phev-systems/ev-on-board-chargers/>
- [4] The beneficials of a 1D-solver
<https://www.femto.eu/stories/1d-system-simulation/>
- [5] Electric Vehicle Control Module (VCU)
<https://conti-engineering.com/components/electric-vehicle-control-module-vcu/>
- [6] Efficiency of electric machines
<https://www.energy.gov/sites/prod/files/2014/04/f15/10097517.pdf>
- [7] Motors, how they work
<https://easyelectriclelife.groupe.renault.com/en/outlook/technology/understanding-the-power-output-of-an-electric-motor/>
- [8] Britannica, T. Editors of Encyclopaedia (2021, April 26). Conservation law. Encyclopedia Britannica. <https://www.britannica.com/science/conservation-law>
- [9] Taler, D. Experimental determination of correlations for average heat transfer coefficients in heat exchangers on both fluid sides. Heat Mass Transfer 49, 1125–1139 (2013). <https://doi.org/10.1007/s00231-013-1148-5>
- [10] White, F. M, Fluid Mechanics 8e in SI Units (Book, 2016),2016,feb

- [11] Chowdhury, S., Leitzel, L., Zima, M., Santacesaria, M. et al., "Total Thermal Management of Battery Electric Vehicles (BEVs)," SAE Technical Paper 2018-37-0026, 2018, doi:10.4271/2018-37-0026.
- [12] Measurements and Error Analysis
https://www.webassign.net/question_assets/unccolphysmechl1/measurements/manual.html Retrieved (2021-05-04)
- [13] Yang, Yinye, et al. "Thermal management of electric machines." IET Electrical Systems in Transportation 7.2 (2016): 104-116.
- [14] Tidblad Lundmark, Sonja, et al. "Vehicle components and configurations." (2013): 22-32.
- [15] <https://www.energy.gov/eere/articles/how-does-lithium-ion-battery-work>
 Retrieved:2021-05-04
- [16] Porsche Engineering Magazine 1/2011 Retrieved (2021-05-04)
- [17] <https://www.hella.com/techworld/uk/Technical/Car-air-conditioning/Thermal-management-in-electric-and-hybrid-vehicles-1725/>
 Retrieved:2021-05-04
- [18] Naveira-Cotta, Carolina P., Renato M. Cotta, and Helcio RB Orlande. "Inverse analysis with integral transformed temperature fields: Identification of thermo-physical properties in heterogeneous media." International Journal of Heat and Mass Transfer 54.7-8 (2011): 1506-1519.
- [19] Dinakar, Pradeep, and Gautham Rajeeve. Modelling and Simulation of Cooling Systems for BEV High Voltage Battery. MS thesis. 2016.
- [20] Incropera, Frank P., et al. Principles of heat and mass transfer. Wiley, 2013.
- [21] https://se.mathworks.com/help/simulink/index.html?s_tid=CRUX_topnav Retrieved:2021-05-06
- [22] <https://www.energy.gov/eere/electricvehicles/electric-vehicle-benefits>
 Retrieved:2021-05-06
- [23] Li, Jiling, and Zhen Zhu. Battery thermal management systems of electric vehicles. MS thesis. 2014.
- [24] <https://cdn2.hubspot.net/hub/103829/file-634817599-pdf/docs/Made-in-CA/made-in-california-manufacturer-specialty-motors-servo-pumping-dispensing-white-paper.pdf>
- [25] Tutuiianu, Monica, et al. "Development of the World-wide harmonized Light duty Test Cycle (WLTC) and a possible pathway for its introduction in the European legislation." Transportation research part D: transport and environ-

ment 40 (2015): 61-75.

[26] Understanding Pump Curves Jim Elsey 06/27/2016

A

Appendix 1

A.1 Source code listing

```
1
2
3 clc
4 clear all
5 %Authors: Noah Wirsen and Babak Heydarnezhad
6 %Emails: nwirsen@gmail.com and babak.heydarnezhad@volvocars.com
7 %Load the pressure drop and heat loss profiles
8
9 load('clngSys_MEP2_AirFlow_Maps')
10 load('DelP_map_SPA2_Yinlun')
11 load('Rad_Air_heat_loss')
12 load('Pump_input')           %Pressure profiles for the pumps
13 load('Components_profile')  %Pressure profiles for the components
14 load('q_loss')              %Power loss in the IEMF,IEMR,ERAD&EFAD
15 load('cp_glyth')           %Temperature dependent Cp-values
16
17 % State, Steady or Transient
18 State = 0 ;                 % 1 = Steady State && 0 = Transient
19 t=500;                       % Time step (if steady)
20
21 % Valve openings
22 V1=1;                         % setting it 1 radiator, 0 bypass
23 V2=0;                         % setting it 1 P2, 0 Bypass
24 V3=1;                         % setting it 1 Bypass,0 Battery
    Circuit
25 V4=0;                         % setting it 1 HVAC, 0 WCOND RAD
26
27 %Pump Speeds
28 N_Climate=100;               % Pump in Climate circuit (%)
29 N_Battery=100;              % Pump in Battery circuit (%)
30 N_Electric=100;             % Pump in Electric circuit (%)
31
32 Fan_Speed_input = 100;       % Radiator Fan Speed (%)
33 T_Ambient_input =35;        % Ambient temp (C)
```

Listing A.1: Input file for the Simulink Model

A. Appendix 1

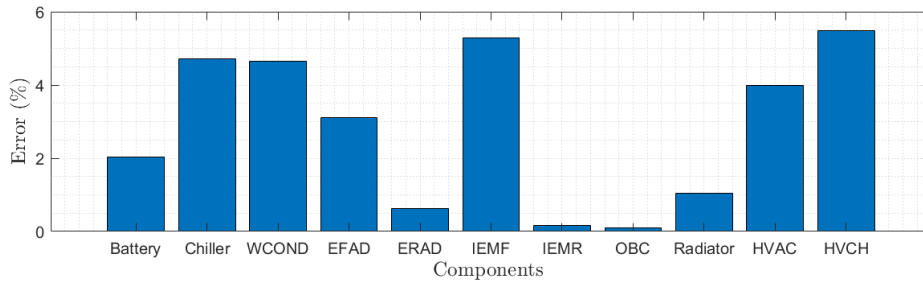


Figure A.1: Error for internal component for 100% pump speed and 0°C ambient temperature

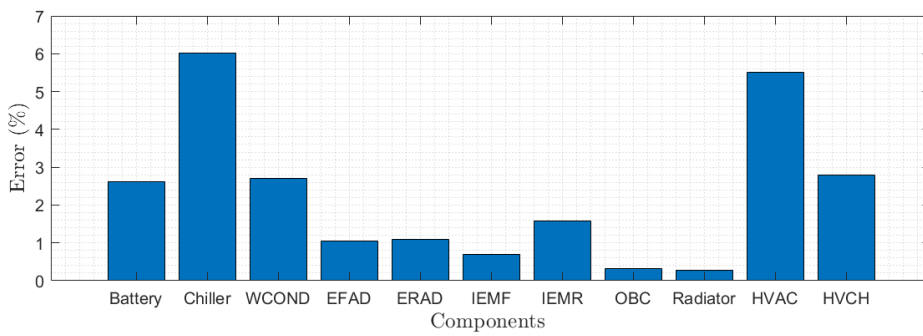
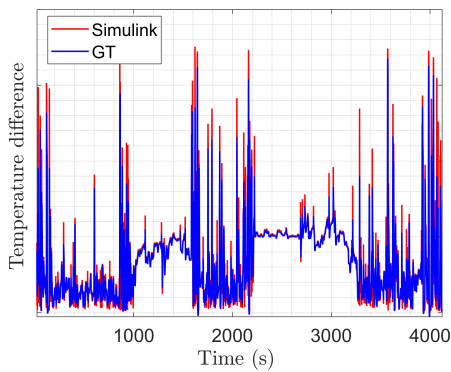
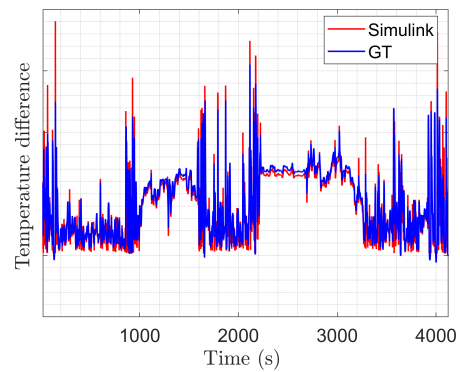


Figure A.2: Error for internal component for 100% pump speed and 40°C ambient temperature



(a) Temperature difference over the front inverter



(b) Temperature difference over the rear inverter

Figure A.3: Temperature difference over the two inverters in Highway 35°C

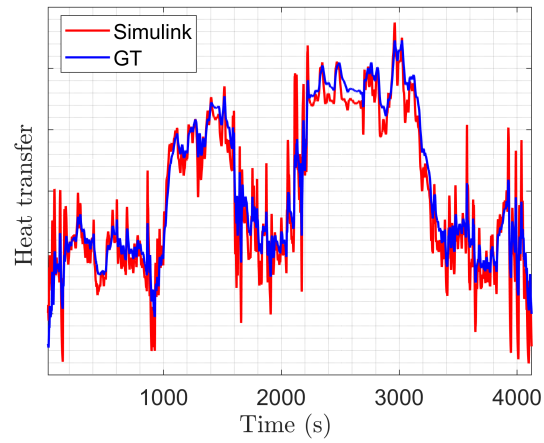


Figure A.4: Heat dissipated in the radiator for highway at 35°C

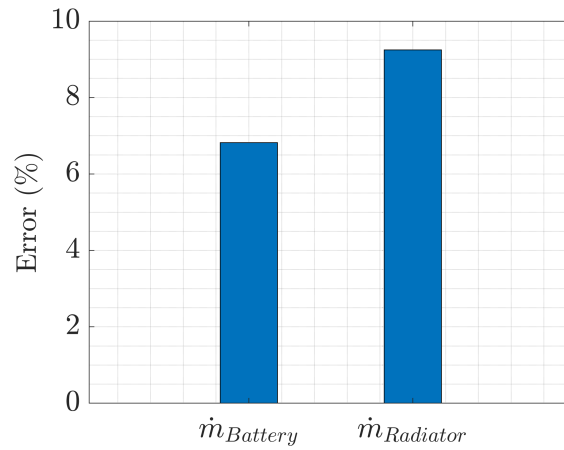


Figure A.5: Mass flow error in radiator and battery for WLTC at 15°C

DEPARTMENT OF MECHANICS AND MARITIME SCIENCES
CHALMERS UNIVERSITY OF TECHNOLOGY
Gothenburg, Sweden
www.chalmers.se



CHALMERS
UNIVERSITY OF TECHNOLOGY